2021 IEEE International Conference on Systems, Man, and Cybernetics (SMC)
17-20 October, 2021. Melbourne, Australia

Symmetry in Biped Walking

Linqi Ye, *Member, IEEE*, Xueqian Wang, *Member, IEEE*, Houde Liu, *Member, IEEE*, and Bin Liang, Senior *Member, IEEE*

2021 IEEE International Conference on Systems, Man, and Cybernetics (SMC) | 978-1-6654-4207-7/21/$31.00 ©2021 IEEE | DOI: 10.1109/SMC52423.2021.9658858

***Abstract*—Symmetry in running was observed by Marc Raibert and was applied to simplify the control of dynamic legged systems. In this paper, we show that symmetry also exists in biped walking and investigate it using two simplified 2D models, that are, the inverted pendulum (IP) model and the linear inverted pendulum (LIP) model, both leading to similar conclusions. To characterize the symmetry in biped walking, the concept of acceleration factor is proposed. Symmetry occurs when the acceleration factor is zero, which results in an unchanged mid-stance velocity. And an important property of symmetry is that the n-step reachable region and the n-step controllable region are exactly the same. This means that if we can achieve speed B from A in n steps, then we can also achieve speed A from B in n steps. Symmetry in walking helps us to better understand human walking and also provides an intuitive way to control robotic walking. As an example, we propose a feedforward controller and a feedback controller, respectively, which can regulate the walking speed very effectively. This work provides us some new insights to view biped walking.**

I. Introduction

The seminal work of Marc Raibert in MIT legged laboratory [1] pioneers the control of dynamical legged locomotion. During his research of a hopping robot, an interesting observation was found, that is, when the robot places its foot on a special location called as "neutral point", it will move on a symmetric trajectory and remain its forward velocity unchanged. Moreover, the robot speeds up when placing its foot ahead of the neutral point and slows down when placing its foot behind the neutral point. This phenomenon was summarized as the symmetry properties in running [2]. Using this property, Raibert designed simple controllers for legged systems range from monopod, biped to quadruped robots, where the symmetry idea plays a crucial role in controlling all of them.

Inspired by Raibert's work, we are thinking about whether the idea of symmetry can be extended to biped walking. However, we find that the robotic groups usually focus on passive walking [3], zero moment point (ZMP) [4], hybrid zero dynamics (HZD) [5], and capture point [6], while symmetry in walking seems to be rarely studied. In contrast, walking symmetry has been widely studied in human and physiological researches. For example, in [7], it is found that the ground reaction forces of healthy individuals exhibit a high degree of symmetry in walking between the left and right limbs. In [8], gait symmetry is expressed as a ratio between the gait values of the left and right limb for step length, stance time, and swing time, and the relation of gait symmetry with age is studied. Moreover, asymmetrical walking is found in patients with nervous system diseases, such as stroke [9], Parkinson [10], and spinal cord injury [11]. Those patients have difficulties in interlimb coordination and thus designing interventions to restore symmetrical walking patterns is important for their rehabilitation.

The aforementioned studies reveal the importance of symmetry in human walking. However, those studies are mostly based on human captured data, but there is a lack of theoretical analysis. Therefore, this paper attempts to study walking symmetry from the mathematical view and finally link it to biped walking control. Running and walking can both be described by simplified models. For example, running can be represented by a spring-loaded inverted pendulum (SLIP) model [12], while walking is usually modeled as an inverted pendulum (IP) [13] or a linear inverted pendulum (LIP) [14]. In IP walking, we keep the stance leg relatively straight in each step, which is the way human prefer to take since it is more energy efficient compared to other walking gaits [15]. While in LIP walking, we bend our knees to keep a constant body height, which can be rarely seen except when people walk gingerly on ice surface to prevent falling. In robotics research, IP walking can be found in related works of passive walking [3] while LIP walking is usually related to ZMP theory [4]. Since IP walking and LIP walking represent two main styles of biped walking, we decide to study walking symmetry based on these two models.

Symmetry in walking affects the velocity transition between steps. It should be noted that the work in [4] have shown some idea of LIP walking very close to the idea of neutral point in running [1], that is, foot placement can determine the moving speed. However, that is not the case for IP walking, in which the speed is dominated by the push off in the end of each step. By proposing the concept of acceleration factor, we find that the symmetry in IP walking and LIP walking can be analyzed in a unified framework.

The main contributions of this work are twofold. First, we extend the symmetry idea in running to walking, thus providing a new perspective to view biped walking. Second, we propose the concept of acceleration factor, which provides

This work was supported by National Natural Science Foundation of China (62003188, 61803221, and U1813216), Guangdong Young Talent with Scientific and Technological Innovation (2019TQ05Z111). *(Corresponding author: Xueqian Wang)*

Linqi Ye is with (1) Artificial Intelligence Institute, Shanghai University, Shanghai 200444, China; (2) Center of Intelligent Control and Telescience, Tsinghua Shenzhen International Graduate School, Tsinghua University, Shenzhen 518055, China (e-mail: ye.linqi@sz.tsinghua.edu.cn).

X. Wang, H. Liu are with the Center of Intelligent Control and Telescience, Tsinghua Shenzhen International Graduate School, Tsinghua University, Shenzhen 518055, China (e-mail: { wang.xq, liu,hd}@sz.tsinghua.edu.cn).

B. Liang is with the Navigation and Control Research Center, Department of Automation, Tsinghua University, 100084 Beijing, China (e-mail: bliang@tsinghua.edu.cn).

a unified framework for the analysis and control of both IP and LIP walking.

The rest of this paper is organized as follows. Symmetry in IP walking and LIP walking are discussed in Section II and Section III, respectively. Then, two kinds of walking speed controllers are proposed in Section IV. Finally, the conclusions are given in Section V.

II. Symmetry in IP Walking

Fig. 1 depicts the IP walking model, which has a point mass on the hip and two massless legs with point feet.

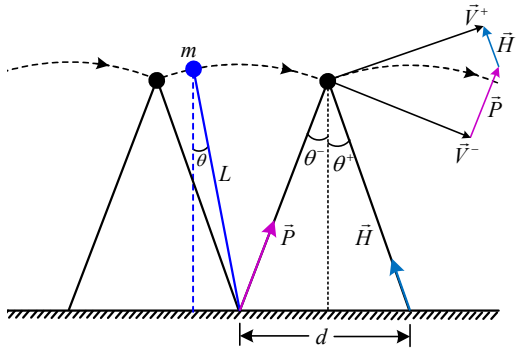

Figure 1. The inverted pendulum (IP) walking model.

During walking, the stance leg maintains a constant length and the center of mass (CoM) moves along an arc. The equation of motion is written as follows

$$\ddot{\theta} = g \sin\theta / L \tag{1}$$

where θ is the stance leg angle, g is the acceleration of gravity, and L is the length of the leg.

When the swing leg touches the ground, it becomes the new stance leg and the previous stance leg starts to swing. During this transition, two ground impulsive forces are exerted to the robot. One is the push off $\vec{P}$ applied to the trailing leg and the other is the heel strike $\vec{H}$ acts on the leading leg (push off is assumed to happen just before heel strike). Using the principle of linear momentum, we have

$$m\vec{V}^{+} - m\vec{V}^{-} = \vec{P} + \vec{H} \tag{2}$$

where $\vec{V}^{+}, \vec{V}^{-}$ are the velocity just after and before switch, respectively. After switch, the former stance leg becomes the new stance leg, so that $\theta^{+} = -\theta^{-}$.

For the IP model, the stance leg are not allowed to leave the ground during walking, so the walking speed is limited by

$$\dot{\theta} \le \sqrt{g \cos\theta / L} \tag{3}$$

During leg transition, the CoM velocity has a sudden change due to the impulsive forces. Fig. 2 shows three cases which represent deceleration, equal-velocity, and acceleration, respectively. In Fig. 2, V_t is the CoM velocity just after push off. By examining the three cases, we find that the velocity transition is directly related to the angle of V_t, which is denoted by α in Fig. 2.

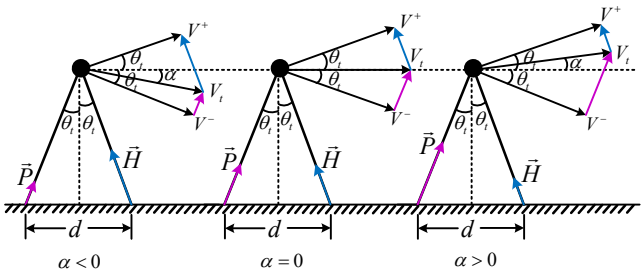

Figure 2. Velocity transition in IP walking. a) α<0 results in deceleration; b) α=0 maintains the same velocity; c) α>0 results in acceleration.

Inspired by Fig. 2, we define the acceleration factor for IP walking as

$$a_{ip} = \tan\alpha = V_t^z / V_t^x \tag{4}$$

which represents the vertical/horizontal component ratio of the CoM velocity and determines the velocity after transition.

Since the ground forces $\vec{P}$ and $\vec{H}$ always point upwards, α is limited by $-\theta_t \le \alpha \le \theta_t$ and the acceleration factor is constrained by

$$-\tan\theta_t \le a_{ip} \le \tan\theta_t \tag{5}$$

where θ_t is the leg angle at transition, which is related to the step length with

$$\theta_t = \text{asin}(d / 2L) \tag{6}$$

Substituting (6) into (5), the relationship between the acceleration factor and the step length is

$$-d / \sqrt{4L^2 - d^2} \le a_{ip} \le d / \sqrt{4L^2 - d^2} \tag{7}$$

Using (7), the feasible range of a_{ip} with respect to different step lengths is drawn in Fig. 3. It can be observed that the upper bound and lower bound of a_{ip} are symmetric about the equal-velocity line.

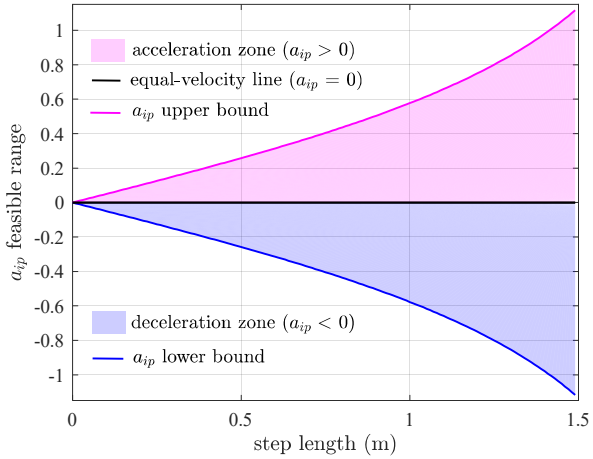

Figure 3. The feasible range of a_{ip} for IP walking.

We can use the mid-stance velocity (when $\theta = 0$) to represent the walking velocity in each step. The relationship

of the mid-stance velocity between two successive steps can be calculated as follows

$$V_{k+1} = \sqrt{\left[V_k^2 + 2gL(1-\cos\theta_t)\right]\frac{\cos^2(\theta_t-\alpha)}{\cos^2(\theta_t+\alpha)} - 2gL(1-\cos\theta_t)} \quad (8)$$

where V_k is the mid-stance velocity of step k, $\alpha = \text{atan}(a_{ip})$, and θ_t is determined by (6).

From (8), it indicates that (d, a_{ip}) (or (θ_t, α)) can be used as a pair of control inputs, which determines the velocity transition between steps. Specially, when $a_{ip} = 0$, we have $V_{k+1} = V_k$, which results in a symmetric gait (see Fig. 4).

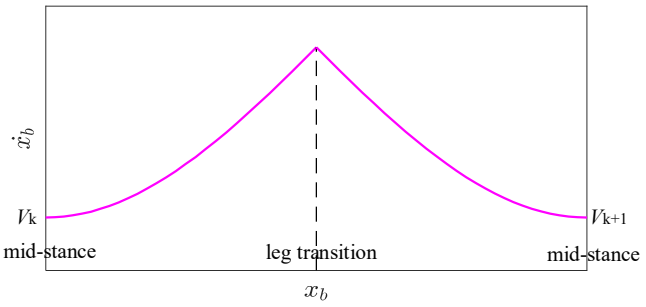

Figure 4. Symmetry in one step for IP walking. x_b represents the absolute horizontal position of the CoM

Besides, we find another symmetry in two steps, that is, if we first take an action pair (d, a_{ip}) in a step and then take $(d, -a_{ip})$ in the next step, the mid-stance velocity will remain unchanged (this can be easily verified from (8)). This results in the symmetry in two steps, which is shown in Fig. 5.

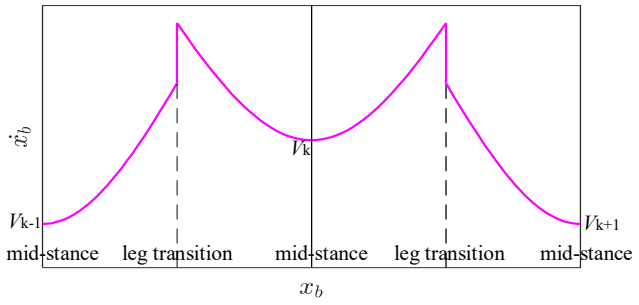

Figure 5. Symmetry in two steps for IP walking.

Furthermore, we investigate the reachable region problem, that is, for a given V_k, to find the boundary of V_{k+1}. Actually, this is an inverse problem of the controllable region concept in [14], which aims to finding all possible values of V_k that can lead to V_{k+1}. Interestingly, we have the following conclusion.

Theorem 1: The reachable region and the controllable region are the same for any given velocity.

Proof: Denote the reachable region and controllable region of V_a as $\boldsymbol{R}^1$ and $\boldsymbol{C}^1$, respectively. Assume that $\boldsymbol{R}^1 \neq \boldsymbol{C}^1$, which means that there is an element V_b in $\boldsymbol{R}^1$ but not in $\boldsymbol{C}^1$. However, if we can achieve V_b from V_a by taking action (d, a_{ip}), then we can also achieve V_a from V_b by taking action $(d, -a_{ip})$. This indicates that V_b should belong to $\boldsymbol{C}^1$, which is contradictory to the assumption that $V_b \notin \boldsymbol{C}^1$. Therefore, the reachable region should always equal to the controllable region. This completes the proof.

We find it difficult to get the explicit expression of the reachable region. However, we have shown in [13] that the maximum reachable velocity can be obtained when the leg transition satisfies $\dot{\theta}/\cos(2\theta) = \sqrt{g\cos\theta/L}$ while the minimum reachable velocity happens when the leg transition satisfies $\dot{\theta} = \sqrt{g\cos\theta/L}$. Therefore we can use numerical methods to obtain the reachable region. We have adopted Matlab's "ode45" function with an event option. For convenience, we denote the reachable region as

$$\boldsymbol{C}^1(V_k) = \left\{V_{k+1} \mid f_{\min}(V_k) \le V_{k+1} \le f_{\max}(V_k)\right\} \quad (9)$$

where $f_{\min}$ and $f_{\max}$ are interpolation functions obtained from the numerical solutions which represent the minimum and maximum reachable velocity, respectively (the minimum reachable velocity is set to zero if it is negative). Using (9), the two-step reachable region can also be obtained, that is

$$\boldsymbol{C}^2(V_k) = \left\{V_{k+1} \mid f_{\min}(f_{\min}(V_k)) \le V_{k+1} \le f_{\max}(f_{\max}(V_k))\right\} \quad (10)$$

and so for the n-step reachable region.

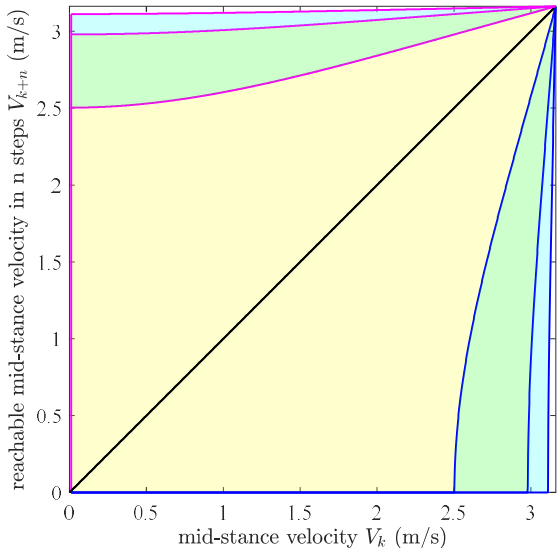

Figure 6. The n-step reachable region for IP walking. The yellow, green, and blue areas represent the 1-step, 2-step, and 3-step reachable regions, respectively.

Fig. 6 shows the n-step reachable region for n = 1, 2, 3 (we have adopted $L = 1\,\text{m}, g = 10\,\text{m/s}^2$). The black line represents the equal-velocity line, which corresponds to $a_{ip} = 0$. Above the black line is the acceleration zone, while under it is the deceleration zone. From Fig. 6, it can be seen that the upper bound and the lower bound of the n-step reachable region are symmetrical about the equal-velocity line, which is actually a visualized representation of Theorem 1. Besides, it can be

observed that the two-step reachable region has covered most of the feasible velocity space (the box area), which validates an interesting observation in [14] that "two steps is enough".

III. Symmetry in LIP Walking

The LIP walking model is depicted in Fig. 7. The difference with IP walking is that the stance leg changes its length to maintain a constant CoM height during walking ($h = 1\text{m}$ is used in this paper). And the leg transition happens in a smooth way where the CoM velocity maintains the same. The double stance phase is also assumed to be instantaneous.

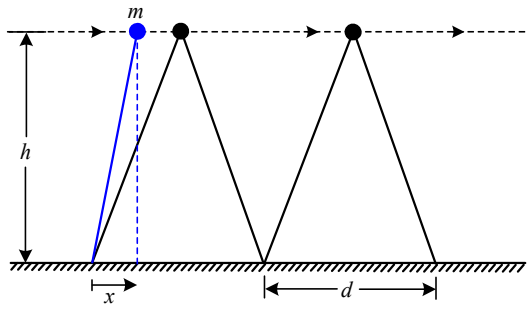

Figure 7. The linear inverted pendulum (LIP) walking model.

During the continuous phase, the system follows the dynamics of a linear inverted pendulum, which is

$$\ddot{x} = gx / h \tag{11}$$

where x is the horizontal position of the hip relative to the stance foot.

In leg transition, the former swing leg becomes the new stance leg, so we have

$$x^+ = x^- - d,\ \dot{x}^+ = \dot{x}^- \tag{12}$$

where d is the step length.

Unlike IP walking, the ground force will never be negative in LIP walking. However, the leg length has a maximum value, which puts the following limits on x

$$x^2 + h^2 \le l_{\max}^2 \tag{13}$$

where $l_{\max}$ is the maximum value of the leg length ($l_{\max} = 1.2\,\text{m}$ is used in this paper). In this paper, we assume that the leg can swing as fast as we want so there are no speed limitation for LIP walking.

Three cases of LIP walking are shown in Fig. 8. Unlike IP walking, the CoM velocity keeps unchanged during leg transition in LIP walking. However, the mid-stance velocity changes if the swing leg and stance leg are asymmetric during leg transition. Therefore, we define the acceleration factor for LIP walking as follows

$$a_{lip} = d_{st} - d_{sw} \tag{14}$$

It can be verified that $a_{lip} = 0$ indicates equal-velocity, $a_{lip} > 0$ indicates acceleration and $a_{lip} < 0$ indicates deceleration, which are the same as in IP walking.

Similarly, the symmetry in LIP walking for one step and two steps are shown in Fig. 9 and Fig. 10, respectively.

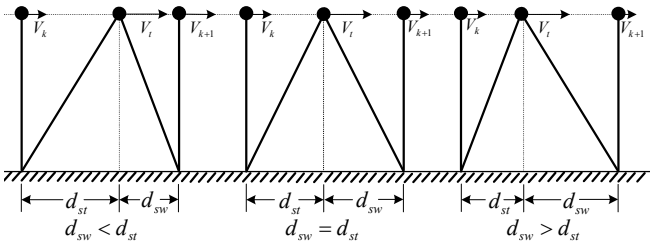

Figure 8. Velocity transition in LIP walking. If $d_{sw} < d_{st}$, the mid-stance velocity increases; if $d_{sw} = d_{st}$, the velocity remains unchanged; if $d_{sw} > d_{st}$, the mid-stance velocity decreases.

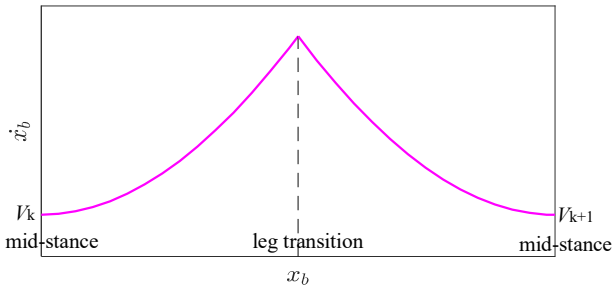

Figure 9. Symmetry in one step for LIP walking.

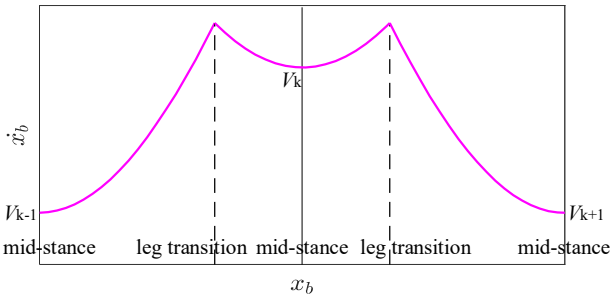

Figure 10. Symmetry in two steps for LIP walking.

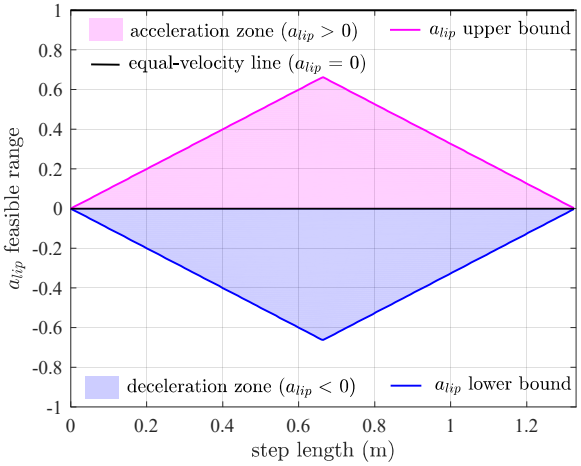

Figure 11. The feasible range of a_{lip} for LIP walking.

We assume that the CoM always locates between the stance foot and swing foot during leg transition. Then the boundary of a_{lip} is

$$\begin{cases} 0 \le a_{lip} \le d, \text{ if } d \le d_m \\ d - 2d_m \le a_{lip} \le 2d_m - d, \text{ if } d > d_m \end{cases} \tag{15}$$

where $d_m = \sqrt{l_{\max}^2 - 1}$ is the upper limit for d_{st} and d_{sw}.

With (15), the feasible range of a_{lip} with respect to different step lengths is drawn in Fig. 11. It can be observed that the upper bound and lower bound of a_{lip} are also symmetric about the equal-velocity line.

For LIP walking, the relationship of the mid-stance velocity between two successive steps is derived as follows

$$V_{k+1} = \sqrt{V_k^2 + gda_{lip} / h} \tag{16}$$

It can be proved that (16) retains the same property as (8) in IP walking so that Theorem 1 still holds. For (16), we can obtain the reachable region explicitly, that is

$$\sqrt{V_k^2 - gd_m^2 / h} \le V_{k+1} \le \sqrt{V_k^2 + gd_m^2 / h} \tag{17}$$

(the minimum reachable velocity is set to zero if $V_k^2 - gd_m^2 / h$ is negative). We draw the n-step reachable region for LIP walking in Fig. 12. It can be observed that the upper bound and the lower bound of the n-step reachable region are also symmetric about the equal-velocity line. The difference to IP walking is, the region is not enclosing anymore, it can extend along both axes (we only show the part within 5 m/s).

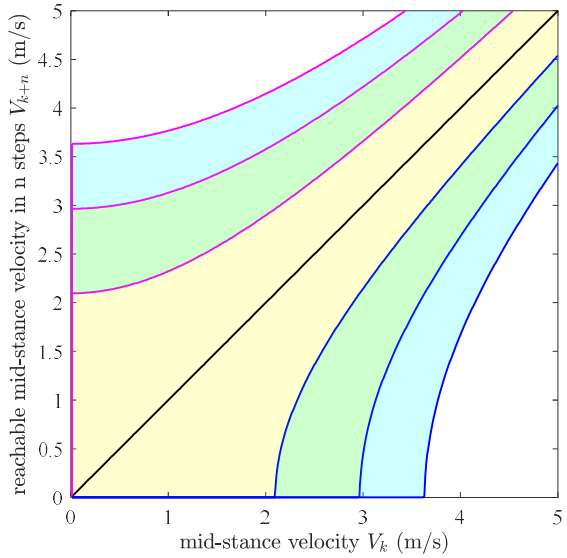

Figure 12. The n-step reachable region for LIP walking. The yellow, green, and blue areas represent the 1-step, 2-step, and 3-step reachable regions, respectively.

IV. Walking Speed Control

Using the results obtained in the previous sections, it becomes easy to design walking controllers to regulate the walking speed. Here we give two examples: a feedforward controller which achieves the desired speed by taking the least steps, and a feedback controller, which gradually regulate the speed to the desired value in a smooth way.

First, the feedforward controller is given in Fig .13. It uses all means (adjust both step length and acceleration factor) to achieve the desired velocity as soon as possible, which is time-optimal (or dead-beat). In this case, the control action pair (d, a) (a represents a_{ip} or a_{lip}) that leads to the maximum/minimum reachable velocity should be precomputed for all velocity.

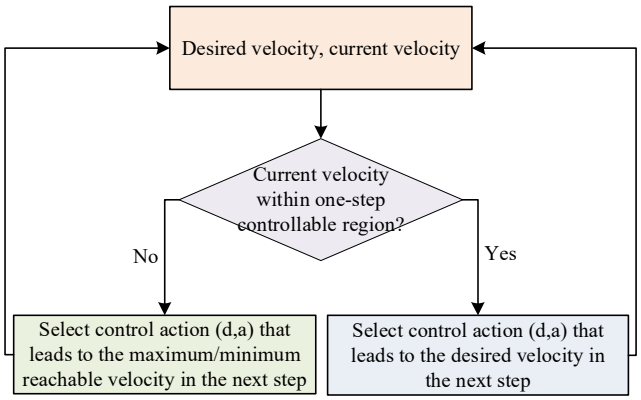

Figure 13. The feedforward controller (for both IP walking and LIP walking).

Next, we design feedback controller which only uses the acceleration factor to regulate the walking speed while the step length can be set freely. The feedback controller for IP walking is designed as follows

$$a_{ip} = a_1 \tanh\left[\lambda_1 (V_r - V_k)\right] \tag{18}$$

where λ_1 is a positive constant and

$$a_1 = d / \sqrt{4L^2 - d^2} \tag{19}$$

And the feedback controller for LIP walking is designed as

$$a_{lip} = a_2 \tanh\left[\lambda_2 (V_r - V_k)\right] \tag{20}$$

where λ_2 is a positive constant and

$$a_2 = \begin{cases} d, \text{ if } d \le d_m \\ 2d_m - d, \text{ if } d > d_m \end{cases} \tag{21}$$

Remark: a_1, a_2 can also be selected as other positive values smaller than the selected values here.

Simulation results are given in Figs. 14~17. It can be seen that the feedforward controller can achieve the desired velocity using minimum steps, i.e., it takes exactly n steps for the initial velocity within n-step controllable region. While the feedback controller takes more steps and converge to the desired velocity gradually. However, the feedback controller is simpler and gives an additional freedom to adjust the step length freely, which is particularly useful when walking on rough terrains with foot placement constraints. In practice, we can decide on which method to be used according to our control goals.

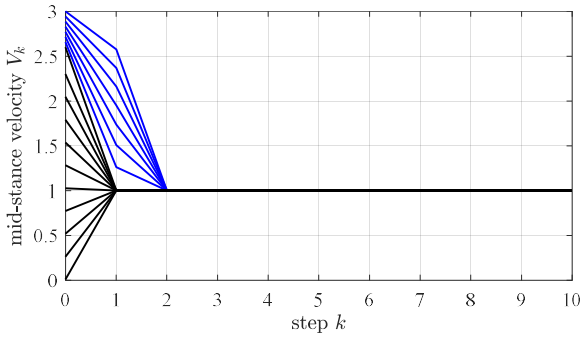

Figure 14. Velocity curve for IP walking using feedforward controller.

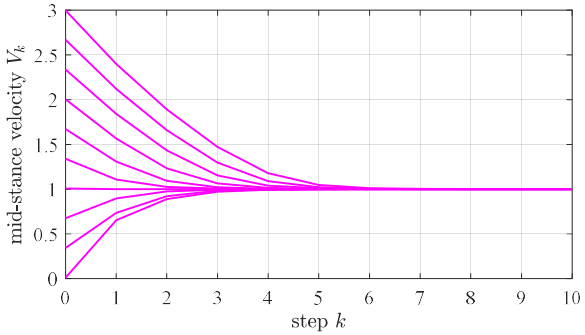

Figure 15. Velocity curve for IP walking using feedback controller. $\lambda_1 = 2, d = 0.6$ are adopted.

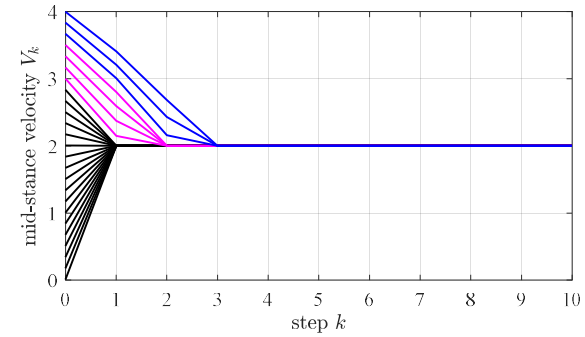

Figure 16. Velocity curve for LIP walking using feedforward controller.

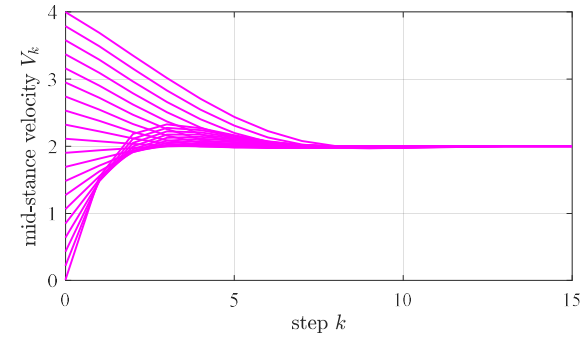

Figure 17. Velocity curve for LIP walking using feedback controller. $\lambda_2 = 0.4, d = 0.6$ are adopted.

V. CONCLUSIONS

Symmetry is widely studied in Mathematica and art, maybe because it provides us a sense of beauty. In legged locomotion, symmetry also plays an important role, which is shown in both running and walking. This work investigates the symmetry in biped walking and builds a unified framework to study the symmetry in both IP walking and LIP walking. When we walk, symmetry usually occurs in steady state of a periodic gait while asymmetry can break this steady state and prompt the transfer to a new periodic gait. Walking asymmetry is also highly related to nervous system diseases. By studying the symmetry in walking and make use of it, we gain more understanding on human walking and also obtain a useful tool to facilitate robotic walking control. Future work will focus on extending this work to 3D walking.

REFERENCES

[1] M. H. Raibert, *Legged robots that balance*. MIT press, 1986.

[2] M. H. Raibert, "Symmetry in running," *Science*, vol. 231, no. 4743, pp. 1292-1294, 1986.

[3] S. Collins, A. Ruina, R. Tedrake, and M. Wisse, "Efficient bipedal robots based on passive-dynamic walkers," *Science*, vol. 307, pp. 1082-1085, 2005.

[4] S. Kajita, H. Hirukawa, K. Harada, and K. Yokoi, *Introduction to Humanoid Robotics*. Heidelberg, Berlin: Springer, 2014.

[5] K. Sreenath, H. W. Park, I. Poulakakis, and J. W. Grizzle, "A compliant hybrid zero dynamics controller for stable, efficient and fast bipedal walking on MABEL," *The International Journal of Robotics Research*, vol. 30, no. 9, pp. 1170-1193, 2011.

[6] T. Koolen, T. De Boer, J. Rebula, A. Goswami, and J. Pratt, "Capturability-based analysis and control of legged locomotion, Part 1: Theory and application to three simple gait models," *The international journal of robotics research*, vol. 31, no. 9, pp. 1094-1113, 2012.

[7] J. Hamill, B. T. Bates, and K. M. Knutzen, "Ground reaction force symmetry during walking and running," *Research Quarterly for Exercise and Sport*, vol. 55, no. 3, pp. 289-293, 1984.

[8] K. K. Patterson, N. K. Nadkarni, S. E. Black, and W. E. McIlroy, "Gait symmetry and velocity differ in their relationship to age," Gait & posture, vol. 35, no. 4, pp. 590-594, 2012.

[9] L. N. Awad, J. A. Palmer, R. T. Pohlig, S. A. Binder-Macleod, and D. S. Reisman, "Walking speed and step length asymmetry modify the energy cost of walking after stroke," *Neurorehabilitation and Neural Repair*, vol. 29, no. 5, pp. 416-423, 2015.

[10] W. Nanhoe-Mahabier, A. H. Snijders, A. Delval, V. Weerdesteyn, J. Duysens, S. Overeem, and B. R. Bloem, "Walking patterns in Parkinson's disease with and without freezing of gait," *Neuroscience*, vol. 182, pp. 217-224, 2011.

[11] M. Kumprou, P. Amatachaya, T. Sooknuan, T. Thaweewannakij, and S. Amatachaya, "Is walking symmetry important for ambulatory patients with spinal cord injury," *Disability and Rehabilitation*, vol. 40, no. 7, pp. 836-841, 2018.

[12] P. M. Wensing and D. E. Orin, "High-speed humanoid running through control with a 3D-SLIP model," in *IEEE/RSJ International Conference on Intelligent Robots and Systems (IROS)*, 2013, pp. 5134–5140.

[13] L. Ye and X. Chen, "Understand Human Walking through a 2D Inverted Pendulum Model," in *IEEE-RAS 18th International Conference on Humanoid Robots* (Humanoids), 2018, pp. 340-345.

[14] P. Zaytsev, W. Wolfslag, and A. Ruina, "The boundaries of walking stability: Viability and controllability of simple models," *IEEE Transactions on Robotics*, vol. 34, no. 2, pp. 336-352, 2018.

[15] M. Srinivasan and A. Ruina, "Computer optimization of a minimal biped model discovers walking and running," *Nature*, vol. 439, no. 7072, pp.72-75, 2006.